

Published in final edited form as:

Arch Oral Biol. 2010 September ; 55(9): 663–669. doi:10.1016/j.archoralbio.2010.05.014.

The Effects of Tooth Extraction on Alveolar Bone Biomechanics in the Miniature Pig, *Sus scrofa*

K. Yeh¹, T. Popowics¹, K. Rafferty², S. Herring^{1,2}, and M. Egbert³

¹ Dept. of Oral Biology, University of Washington, Seattle, WA 98195

² Dept. of Orthodontics, University of Washington, Seattle, WA 98195

³ Division of Oral and Maxillofacial Surgery, Children's Hospital and Regional Medical Center, Seattle, WA 98195

Abstract

Objective—This study investigated the role of occlusion in the development of biomechanical properties of alveolar bone in the miniature pig, *Sus scrofa*. The hypothesis tested was that the tissues supporting an occluding tooth would show greater stiffness and less strain than that of a non-occluding tooth.

Design—Maxillary teeth opposing the erupting lower first molar (M₁) were extracted on one side. Occlusion developed on the contralateral side. Serially administered fluorochrome labels tracked bone mineralization apposition rate (MAR). A terminal experiment measured *in vivo* buccal alveolar bone strain on occluding and non-occluding sides during mastication. *Ex vivo* alveolar strains during occlusal loading were subsequently measured using a materials testing machine (MTS/Sintech). Whole specimen stiffness and principal strains were calculated.

Results—MAR tended to be higher on the extraction side during occlusion. *In vivo* buccal shear strains were higher in the alveolar bone of the occluding side vs. the extraction side (mean of 471 με vs. 281 με, respectively; p=0.04); however, *ex vivo* shear strains showed no significant differences between sides. Stiffness differed between extraction and occlusion side specimens, significantly so in the low load range (344 vs. 668 MPa, respectively; p=0.04).

Conclusions—Greater *in vivo* shear strains may indicate more forceful chews on the occluding side, whereas the similarity in *ex vivo* bone strain magnitude suggests a similarity in alveolar bone structure and occlusal load transmission regardless of occlusal status. The big overall change in specimen stiffness that was observed was likely attributable to differences in the periodontal ligament rather than alveolar bone.

1. Introduction

Alveolar bone formation and maintenance is thought to rely on the presence of erupting and functioning teeth. The alveolus develops with tooth eruption, including the alveolar bone proper for periodontal ligament attachment, and the surrounding cancellous bone and cortical plates for overall tooth support. Jaws without erupting teeth never develop alveolar

Corresponding author: Tracy Popowics, Box 357132, Dept. of Oral Biology, University of Washington, Seattle, WA 98195, Fax: (206) 685-3162, Phone: (206) 221-5350, Popowics@u.washington.edu.

Publisher's Disclaimer: This is a PDF file of an unedited manuscript that has been accepted for publication. As a service to our customers we are providing this early version of the manuscript. The manuscript will undergo copyediting, typesetting, and review of the resulting proof before it is published in its final citable form. Please note that during the production process errors may be discovered which could affect the content, and all legal disclaimers that apply to the journal pertain.

processes and consist only of basal bone (1,2). Experimental and finite element studies of the loaded tooth and periodontium indicate that the periodontal ligament deforms during occlusal loading and subsequently transmits loads to adjacent bone (3,4). The loading environment of alveolar bone, as well as the bone's response to load, however, remain uncharacterized. This study investigates the properties of alveolar bone and the consequences of removal of occlusal load.

Experimental studies have indicated that alveolar bone is likely to receive multiple sources of load. In addition to the occlusal stresses translated from the immediately adjacent tooth and periodontal ligament, loads arise from more remote origins, such as the occlusion of more distant teeth and the activity of masticatory muscles. *In vivo* measurement of strain in the mandibular body during chewing in pigs, rabbits and primates (5–10) shows a pattern that fits a model of mandibular torsion during mastication. In these previous studies, strain gages were placed on the basal bone of the mandible; thus strain in the alveolar region during mastication remains unmeasured.

This study was undertaken to understand the mechanical properties and functioning of alveolar bone and to test the hypothesis that the tissues supporting an occluding tooth would show greater stiffness and less strain than those of a non-occluding tooth. The rationale behind this hypothesis was that removal of antagonist teeth would remove the primary source of load from alveolar bone, and that when present, this load causes alveolar bone to adapt by fortification against occlusal stresses.

2. Materials and Methods

Animal Procedures

All procedures were humane and approved by the University of Washington Animal Care and Use Committee. In 6 female Hanford miniature pigs, maxillary teeth opposing the mandibular first molar, M_1 , on one side were extracted so that M_1 erupted unopposed. Prior to tooth extraction, lateral cephalograms were taken to establish the positions of the target teeth (unerupted upper first molar, M^1 , and erupted deciduous upper fourth premolar, dp^4) within the maxilla. Tooth extraction surgeries were performed in an aseptic facility. Animals were anesthetized by mask using isoflurane in oxygen and an endotracheal tube was established. The pig was positioned on its back and a mouth prop was placed between posterior teeth. For M^1 , the gingiva was reflected to expose the dental follicle for extraction. For dp^4 , a dental drill was used to section the tooth crown sagittally into mesial and distal parts for easier tooth removal. Following removal of teeth, the gingival flaps overlying M_1 were sutured. Antibiotics (ampicillin) and analgesics (buprenorphine and fentanyl) were administered prior to, and on a daily basis during the recovery period.

Lateral cephalometric films and dental impressions were made in order to track the eruption of M_1 and the development of M^1/M_1 occlusion on the non-extraction side (Table 1, Figure 1). In the first week after arrival, pigs were x-rayed to determine whether the eruption of M^1/M_1 was at the mucosal penetration stage. If not, subsequent experiments were delayed. In pigs with M^1/M_1 eruption confirmed at the mucosal penetration stage, extraction of one side dp^4 and M^1 were performed the following week. The side of extraction was randomly determined. Subsequent tooth eruption and occlusal development on the non-extraction side M^1/M_1 were checked by x-ray and dental impressions before proceeding to the following steps. Impression trays were constructed to fit the upper and lower dental arches (TRIAD, TruTray, Dentsply International Inc.). Impressions were made on anesthetized pigs using alginate (Jeltrate, Dentsply International Inc.). Dental stone casts were poured and examined for cusp attrition as an indication of occlusal function.

Electromyography (EMG) was used to track the chewing activity before and after tooth extraction (Table 1). Pigs were trained to eat pelleted pig chow in the laboratory in order to familiarize them with the experimental environment. Surface EMG electrodes were attached to the skin surface of bilateral temporalis and masseter muscles. A ground electrode was attached to the skin overlying the frontal bone. Pigs were awakened and allowed to eat freely during EMG recordings. Baseline EMGs were collected prior to tooth extraction, as well as the week after extraction and subsequently every two weeks. The chewing side was judged for each chew based on the EMG activity of the masticatory muscles. Late masseter muscle activity determined the working side for that chew (7).

A terminal procedure to measure alveolar strain was carried out following the development of M_1 occlusion (Table 1). Pigs were anesthetized by mask with isoflurane and nitrous oxide. A small incision was made buccally to access the buccal alveolar bone supporting the mandibular first molar (M_1). The alveolar periosteum was reflected, the bone surface was prepared for strain gage adhesion, and rosette strain gages (Tokyo Sokki Kenyujo Co., Ltd.; FRA-1-11) were glued to the bone. All strain gages were balanced prior to attachment, as well as following attachment but prior to data collection. Strain gage wires exited through the buccal incision and this incision was sutured. This procedure was followed on both right and left sides of the mandible. Additionally, surface EMG electrodes were attached to skin overlying the temporalis and masseter muscles bilaterally. After the administration of analgesics (ketorolac and buprenorphine) the pig was allowed to awaken. The pig fed enthusiastically and alveolar strain and EMG were recorded at 500Hz using the MP100 System and Acqknowledge software (Biopac Systems Inc., Goleta, CA). Following data recording, the pig was reanesthetized and subsequently euthanized.

Ex Vivo Testing

Segments from 5 of the pigs were prepared from right and left side mandibles as described in Popowics et al. (2009). The segments included M_1 and surrounding periodontal tissue, as well as the posterior region of the deciduous fourth premolar, dp_4 . The occlusal surface of M_1 was ground flat with a dental drill in order to support even loading of the tooth, and the dp_4 was ground to a lower level for focused loading on M_1 . Rosette strain gages from *in vivo* testing were maintained on the buccal alveolar surface and were subsequently used for *ex vivo* strain measurement. Additional gages were affixed posterior to M_1 on the anterior wall of the M_2 crypt, and on the lingual cortical plate adjacent to the distal M_1 cusps. The occlusal surface of M_1 was loaded in compression at 0.3mm/s until 890N using a materials testing machine (MTS/Sintech). This loading rate was selected to approximate the 2–3 Hz chewing rate of minipigs. The 890N endpoint was selected as a load level likely to be in the upper range of normal bite force in occluding molar teeth (11). A saline drip was used to maintain specimen moisture. Occlusal tape was placed over M_1 and was checked between tests to verify that the crown bore the compressive load. A series of five cycles was performed sequentially in order to precondition the specimen, and the data from the sixth cycle were used for comparison of overall specimen stiffness and alveolar strain. Applied stresses were estimated by dividing compressive loads by the M_1 cross-sectional area. Overall specimen strains were calculated as the change in distance between compression platens divided by the pre-test distance. In order to compare the slope of the stress-strain curves with a previous study (4), the slope of the stress-strain curve was calculated between 200–440N (low load stiffness). Additionally, the slope between 445–890N represented stiffness within the high load range (high load stiffness). Strain gage measurements of alveolar strain were recorded simultaneously with occlusal loading and principal strain magnitudes were calculated at 440N and the 890N loading endpoints.

Mineralization

In 5 of the pigs, four different fluorescent bone markers were used to measure bone apposition rate in association with tooth eruption. The first bone marker (calcein, 12.5mg/kg dissolved in saline and neutralized to a pH of 7.4) was administered intravenously immediately following tooth extraction (Fig. 1A). At 2 weeks postsurgery, during the emergence of the non-extraction side M1/1 from the gingivae (Fig. 1B), the second bone marker (alizarin red, 30mg/kg dissolved in saline) was injected. At 4 weeks postsurgery, corresponding with the occlusion of non-extraction side M¹/₁ mesial cusps, the third bone marker (tetracycline, 30mg/kg dissolved in saline) was injected (Fig. 1C). The last bone marker (demeclocycline, 12.5mg/kg dissolved in saline) was delivered at 6 weeks postsurgery when the non-extraction side M¹/₁ achieved full occlusal contact (Table 1 and Fig. 1D).

Following mechanical testing, specimens were dehydrated with increasing concentration of ethanol and embedded in methylmethacrylate resin (Microbed, EMS, Fort Washington, PA) without decalcification. UV light (365 nm) was used to cure the methylmethacrylate to polymerization. The cured blocks were attached to plastic stubs with epoxy glue. A circular saw microtome (Leica SP1600, Germany) was used to section the block parasagittally into 50µm thick sections. Sections were mounted on slides with DPX mounting medium (Fluka, Switzerland) and viewed with a fluorescent light microscope (Nikon Eclipse E400, Japan). Three sequential sections containing dp₄ and the mesio-buccal and disto-buccal roots of M₁ were measured and averaged.

Image analysis was performed with MetaVue software (Universal Imaging Corp., Downingtown, PA). The center of each bone mark was first identified. The distance between 1st and 2nd bone marker centers along the axis of bone growth was divided by the duration between injections as the prefunctional mineral apposition rate (MAR). The distance between 3rd and 4th bone marker centers along the axis of bone growth was measured and divided by the duration between injections as the functional MAR. The distance from the center of the fourth bone marker to the top of the osteoid along the axis of bone growth was also measured and divided by the number of days between the last injection to sacrifice as the MAR under full occlusal contact. Three locations, including the alveolar bone between dp₄ and M₁ (M₁ mesial), the interradicular bone of M₁, and the alveolar bone distal to M₁ were measured.

Parametric and non-parametric tests (SPSS 15.0, SPSS Inc., Chicago, IL) were used to compare the differences between occluding and non-occluding corresponding parameters. A p value of less than 0.05 was considered significant.

3. Results

Masticatory EMG and strain

Summaries of chewing side based on EMG data are presented in Table 2. Baseline chewing activity was not recorded for pigs 4565 and 4744 due to technical difficulties. The percentage of chews on each side prior to tooth extraction ranged from 42–55%; thus, percent chewing of approximately 40–60% on each side was defined as normal. At 1–2 weeks following tooth extraction surgeries, all of the pigs showed bias in their chewing movements toward the occluding, non-extraction side of the dentition. By 5–6 weeks post extraction, most pigs showed a more normal masticatory pattern.

Measurements of buccal alveolar bone strain during mastication are given in Table 3. Regardless of chewing side, strains did not differ; thus, data from right and left side chews were combined. Simultaneous measurement of buccal strain on the occlusion and extraction

sides was recorded in 4 pigs, whereas strain measurements from 2 pigs (5536, 4744) were not simultaneous but made from different chewing sequences. In pig 5545 only occlusion side buccal alveolar strain was recorded due to technical difficulties with the extraction side strain gage, and this pig was excluded from paired statistical tests. Mean maximum (ϵ_1) and minimum (ϵ_2) principal strains were similar on the occlusion and extraction sides ($226\mu\epsilon$ and $-245\mu\epsilon$ vs. $198\mu\epsilon$ and $-155\mu\epsilon$, respectively), but when the mean shear strain was calculated as $\epsilon_1 - \epsilon_2$ the occlusion side was significantly higher than the extraction side ($471\mu\epsilon$ vs. $281\mu\epsilon$; $p=0.04$, Wilcoxon signed rank test). Minimum principal strain orientations did not differ between sides. Postmortem examination of occluding side M^1 's showed substantial wear, whereas attrition was absent from extraction side M^1 's.

Total specimen stiffness

Stress-strain curves for the *ex vivo* compressive loading of occluding and extraction side mandibular specimens were distinct (Fig. 2). On the occluding side, the specimens initially showed low stiffness, but stress increased steadily within the 200–440N range, which produced 1–2 MPa of stress on M_1 . The curve continued to rise steeply past 2MPa and reached its steepest level in a linear region within the high load range (3.5–4 MPa). In contrast, the extraction side specimens showed more extensive deformation during early loading and this greater deformation progressed through the low load range. Despite some unevenness, a linear region of increased stress occurred within the high load range. The slopes at low load were significantly greater in occluding than in extraction side specimens (mean stiffness of 668 vs. 344 MPa.; Wilcoxon signed rank test $p= 0.04$, Table 4). On the other hand, the slopes at high load did not differ (Table 4).

Ex vivo strain gage measurements

During *ex vivo* compressive loading at either the 440N or the maximum loading point (890N), strain magnitudes from extraction side specimens generally did not differ significantly from those on the occlusion side (Table 5). For the buccal gage, minimum principal strains (ϵ_2) at 440N ranged from -96 to $-504\mu\epsilon$ and at 890N from -170 to $-900\mu\epsilon$ on each side. In contrast the maximum principal strains (ϵ_1) were lower, ranging from 7 to $106\mu\epsilon$ at the low load point and were approximately double at the high load point, ranging from 20 to $200\mu\epsilon$. Strain magnitudes for the Max (ϵ_1) at 890N differed significantly between extraction and occluding sides ($p=0.04$), however, because the maximum principal strains were low magnitude, and had little effect on shear strain they are unlikely to be biologically significant.

Lingual and crypt strain magnitudes were also generally lower at the 440N load point than the 890N load point (Table 5). No differences between occluding and extraction sides could be detected.

Mineralization

Mineral apposition rate (MAR) analysis was based on measurements from 4 pigs, due to a technical error in specimen preparation of one animal (Table 6.). This small sample size, plus substantial variation, resulted in low power to detect real differences. Nevertheless it is notable that prefunctional MAR was similar on the two sides, with the occluding side showing slightly higher means at two of the three sites measured. At every subsequent time period, however, and at every site, the extraction side showed greater MAR, nearly significant in one comparison (Functional MAR, mesial location, $p=0.06$).

4. Discussion

Maxillary tooth extractions clearly altered masticatory function during M_1 tooth eruption and occlusal development, and removed one source of load from M_1 alveolar bone. Immediately following the unilateral M^1 and dp^4 extractions, pigs favored chewing on the non-extraction side. At this early stage of M_1 eruption, the occluding side M_1 had not yet reached occlusion, thus the preference for non-extraction side chewing likely was an avoidance of the contralateral wound site. With continued M_1 eruption and occlusal contact on the non-extraction side, most pigs recovered a chewing style that used both sides almost equally. Nevertheless, alveolar strains recorded during mastication at the end of the study were greater on the occluding side. These higher occlusion side strains are likely to reflect direct loading of M_1 and could indicate more forceful chews on the occlusion side. It is important to note that pigs have bilateral occlusion, with both sides normally in contact regardless of the side of chewing (12).

Although maxillary extractions removed a major source of M_1 load, substantial strain was present still in the alveolar bone supporting unopposed M_1 's indicating loading from a source other than M_1 occlusion. Both extraction and occlusion sides showed a balance of mean maximum and minimum principal strains, suggesting a similar pattern of torsional deformation. These alveolar strains were similar in magnitude to those recorded in a previous study at a location on the mandibular corpus below dp_4 (7). This previous study proposed that masseter activity in conjunction with occlusion of anterior teeth could twist the mandible during chewing; in the present study, such twisting could account for the strain levels in alveolar bone supporting nonoccluding teeth.

Although measurements of *in vivo* strain and muscle activity suggest changes in usage of occluding and extraction side M_1 's, under identical loads *ex vivo* measurements of alveolar strain showed no differences at any of the three gage locations. The presence of similar strain levels when the load is kept constant indicates that these alveolar regions were equally stiff. These results contradict our original hypothesis that alveolar bone supporting occluding teeth would show greater stiffness and less strain. Evidently, strain generated through more remote loading sources, such as occlusion of surrounding teeth and contraction of masticatory muscles, is sufficient to promote alveolar stiffness in unopposed teeth. The specific deformation of cancellous bone within the alveolar processes remains unknown, although potential differences could be explored using the finite element method (13).

In support of our original hypothesis, differences in whole specimen stiffness were observed; however these differences indicate discrepancies in PDL transmission capacity rather than in alveolar bone deformation. The stress/strain curves showed significant differences at low load levels at which pigs typically chew (200–560N (11)). This stiffness of the occluding side (668 ± 183 MPa) compares well to baseline values for this range of stress seen in previous studies by others (534 MPa (14)), whereas the stiffness of the extraction side was clearly lower (344 ± 101 MPa). Because the PDL acts as a shock absorber, dampening occlusal loads prior to transmitting them to the surrounding bone, the early part of the stress/strain curve is likely to represent PDL deformation, whereas the later portion of the curve with higher stiffness is likely to reflect the recruitment of alveolar bone. The PDL may be less mature in the unopposed extraction side M_1 's than in the occlusion side, contributing to greater deformation on the extraction side. In a previous study, such a discrepancy in PDL development between erupting M_1 's and occluding M_1 's was also thought to account for differences in stiffness during *ex vivo* compression (4).

Lastly, alveolar bone mineralization was not higher when the molars were in occlusion. Rather, bone growth fortified the tooth regardless of occlusal status. In fact, the extraction side showed a tendency for greater mineralization, which may have been due to supra-eruption. An increase in vertical height of alveolar bone associated with unopposed teeth has been observed in mice and rats (15,16). Comparable levels of mineralization between sides in this study are consistent with the finding of similar magnitudes of *ex vivo* alveolar strain.

Acknowledgments

Supported by NIH/NIDCR DE015815.

References

1. Marks SC, Schroeder HE. Tooth Eruption: Theories and Facts. *Anat Rec* 1996;245:374–393. [PubMed: 8769674]
2. Dixon, AD.; Hoyte, DAN.; Ronning, O. Fundamentals of Craniofacial Growth. New York: CRC Press; 1997.
3. Kaewsuriyathumrong C, Soma K. Stress of tooth and PDL structure created by bite force. *Bull Tokyo Med Dent Univ* 1993;40:217–232. [PubMed: 8275547]
4. Popowics T, Yeh KD, Rafferty K, Herring S. Functional cues in the development of osseous tooth support in the pig, *Sus scrofa*. *J Biomech* 2009;42:1961–1966. [PubMed: 19501361]
5. Herring SW, Rafferty KL, Liu Z-J, Marshall CD. Jaw muscles and the skull in mammals: the biomechanics of mastication. *Comp Biochem and Phys* 2001;131(Part A):207–219.
6. Liu ZJ, Herring SW. Bone surface strains and internal bony pressures at the jaw joint of the miniature pig during masticatory muscle contraction. *Arch Oral Biol* 2000;45:95–112. [PubMed: 10716614]
7. Liu Z-J, Herring SW. Masticatory strains on osseous and ligamentous components of the temporomandibular joint in miniature pigs. *J Orofac Pain* 2000;14:265–278. [PubMed: 11203760]
8. Hylander WL. Mandibular function in *Galago crassicaudatus* and *Macaca fascicularis*: an *in vivo* approach to stress analysis of the mandible. *J Morph* 1979;159:253–296. [PubMed: 105147]
9. Hylander WL, Johnson KR, Crompton AW. Loading patterns and jaw movements during mastication in *Macaca fascicularis*: a bone-strain, electromyographic and cineradiographic analysis. *Amer J Phys Anth* 1987;72:287–314.
10. Weijjs WA, de Jongh HJ. Strain in mandibular alveolar bone during mastication in the rabbit. *Arch Oral Biol* 1977;22:667–675. [PubMed: 272139]
11. Bousdras VA, Cunningham JL, Ferguson-Pell M, Bamber MA, Sindet-Pedersen S, Blunn G, et al. A novel approach to bite force measurements in a porcine model *in vivo*. *Int J Oral Maxillofac Surg* 2006;35:663–667. [PubMed: 16540289]
12. Rafferty K, Herring SW, Marshall CD. Biomechanics of the rostrum and the role of facial sutures. *J Morph* 2003;257:33–44. [PubMed: 12740894]
13. Meswania JM, Bousdras VA, Ahir SP, Cunningham JL, Blunn GW, Goodship AE. A novel closed-loop electromechanical stimulator to enhance osseointegration with immediate loading of dental implant restorations. *Proc IMechE Part H: J Engineering in Medicine* 2010;224:1–12.
14. Dorow C, Krstin N, Sander F-G. Determination of the mechanical properties of the periodontal ligament in a uniaxial tensional experiment. *J Orofac Orthop* 2003;64(2):100–107. [PubMed: 12649706]
15. Holliday S, Schneider B, Galang MT, Fukui T, Yamane A, Luan X, et al. Bones, teeth, and genes: a genomic homage to Harry Sicher's "Axial movement of teeth". *World J Orthod* 2005;6:61–70. [PubMed: 15794043]
16. Ejiri S, Toyooka E, Tanaka M, Anwar RB, Kohno S. Histological and histomorphometrical changes in rat alveolar bone following antagonistic tooth extraction and/or ovariectomy. *Arch Oral Biol* 2006;51:941–50. [PubMed: 16814741]

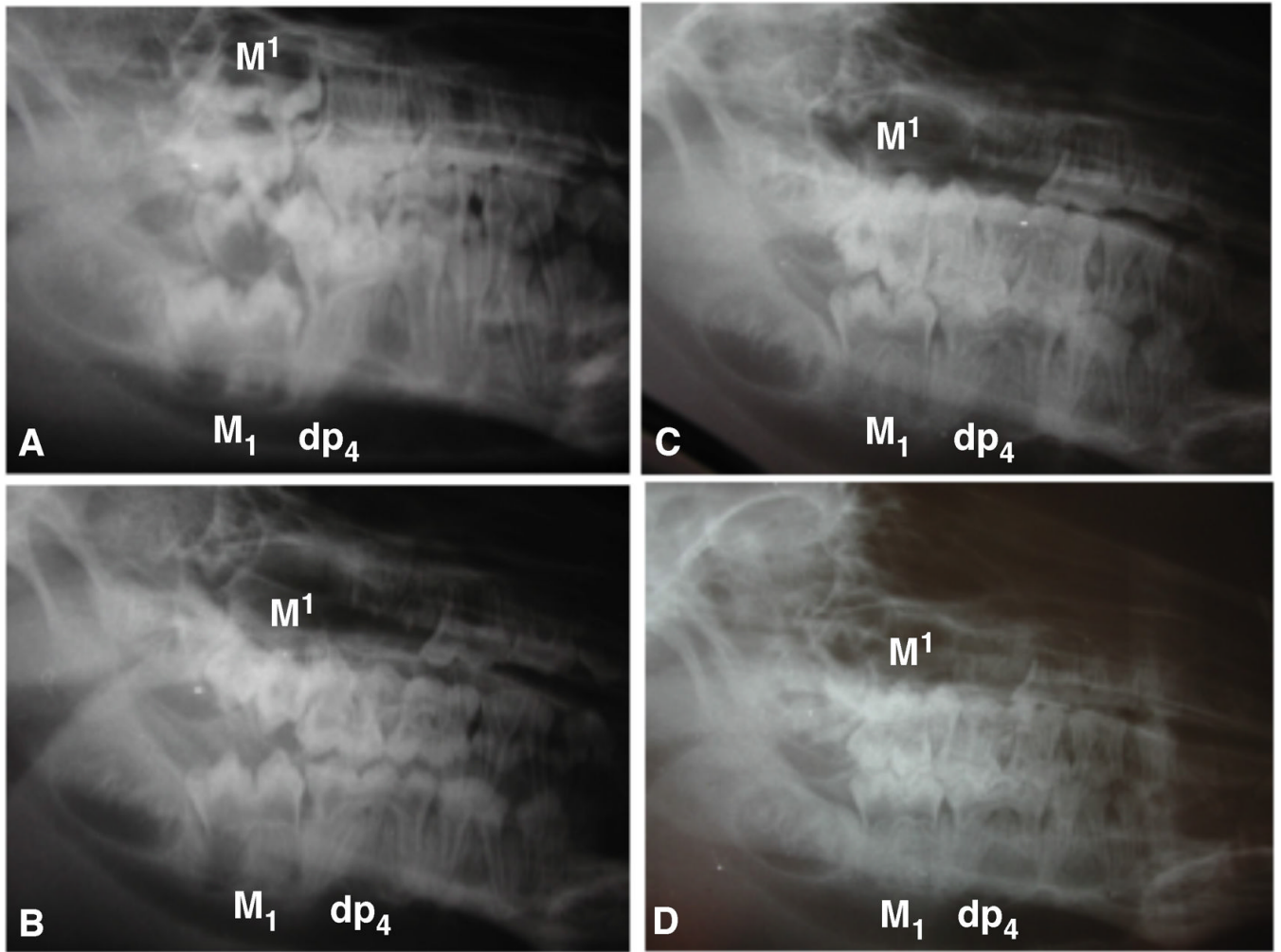


Figure 1.

Lateral cephalograms showing the progressive development of first molar occlusion on the non-extraction side. A. Mesial cusps of M^1 and M_1 have begun to penetrate the overlying mucosa (13 weeks of age). B. Continued emergence of M^1/M_1 mesial cusps from the gingivae (2 weeks post extraction, 16 weeks old). C. Mesial cusps of M^1/M_1 are occluded, while the distal cusps have not yet emerged from the gingiva (4 weeks post tooth extraction, 18 weeks old). D. Distal cusps of M^1 are almost fully occluded with M_1 (6 weeks post tooth extraction, 20 weeks old).

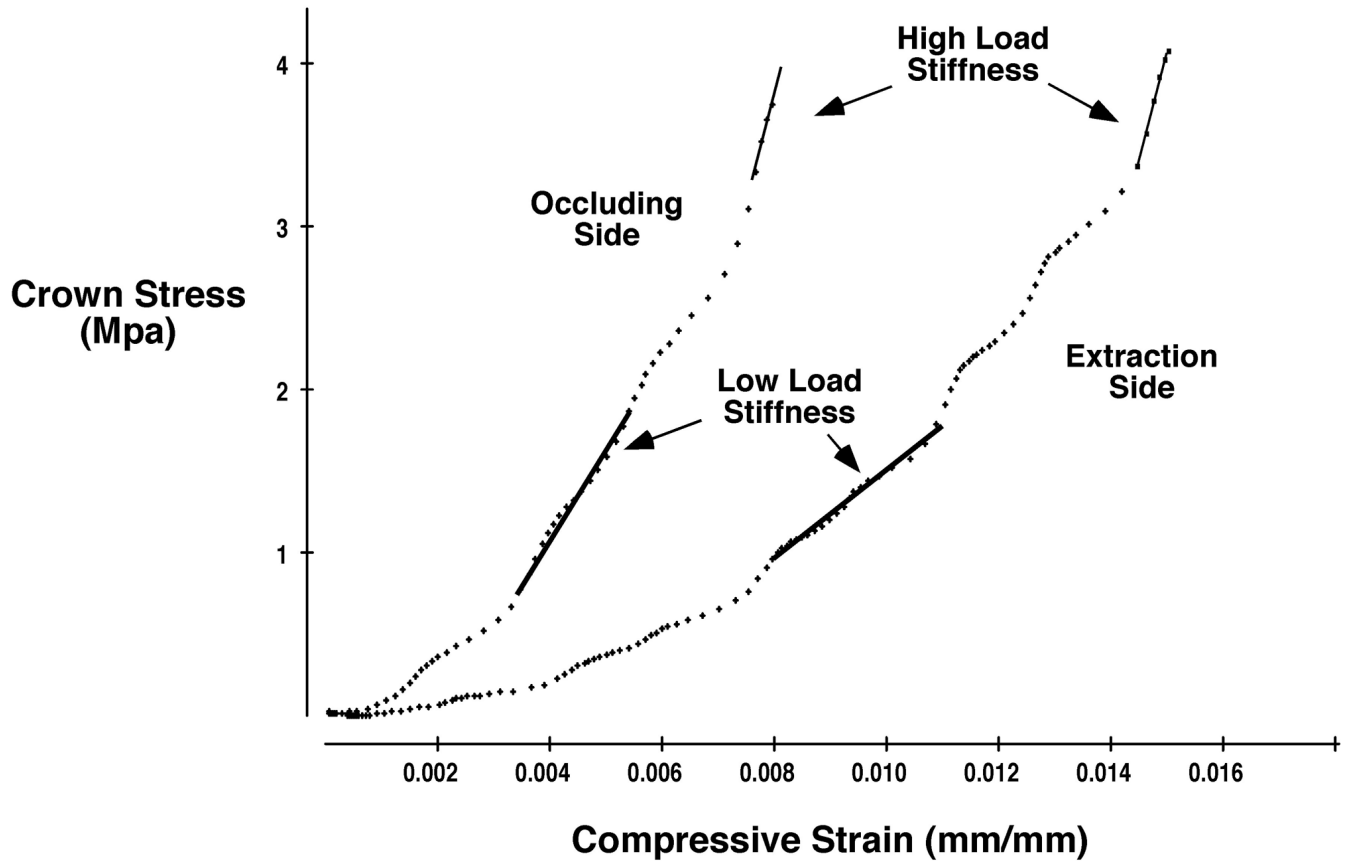


Figure 2. Typical stress-strain curves from compressive loading of occluding and extraction side M₁ specimens from fig 5545. The occluding side specimen showed less deformation at low load than the extraction side specimen.

Table 1
 summary of the approximate stages of occlusal development and experimental progression.

Age*	12-13 wks	14 wks	16 wks	18 wks	20 wks	22-23 wks
Occlusal Stage	M ^{1/1} unerupted	M ^{1/1} mucosal penetration beginning	M ^{1/1} emerging from gingivae; no occlusion	Non-extraction side M ^{1/1} mesial cusps occlude	Non-extraction side M ^{1/1} mesial and distal cusps occlude	Same as 20 wks
Experimental Procedures	Pig Arrival; Radiograph Training EMG	Unilateral dp ⁴ , M ¹ extraction; 1 st bone label (Calcein)	2 nd bone label (Alizarin red); Radiograph; Dental impression	3 rd bone label (Tetracycline); Radiograph; Dental impression	4 th bone label (Demeclocycline); Radiograph; Dental impression	<i>In vivo</i> strain; EMG; Euthanization Post-terminal: <i>In vitro</i> strain; Specimen stiffness; Sectioning

*Exact ages of individual pigs varied for each occlusal development stage.



Table 2
 Chewing on occlusion and extraction sides based on the pattern of muscle activity in EMG recordings (cycle numbers).

Pig	Before Extraction			1-2 Wks Post Extraction			5-6 Wks Post Extraction		
	Occluding	Extraction	Unclear	Occluding	Extraction	Unclear	Occluding	Extraction	Unclear
5398	31 (54%)	26 (46%)	0	44 (64%)	21 (30%)	4 (6%)	61 (55%)	48 (44%)	1 (1%)
5414	41 (55%)	32 (43%)	2 (2%)	57 (77%)	17 (23%)	0	89 (51%)	75 (43%)	9 (6%)
5536	37 (51%)	35 (49%)	0	38 (78%)	9 (18%)	2 (4%)	90 (63%)	54 (37%)	0
5545	43 (54%)	33 (42%)	3 (4%)	33 (79%)	9 (21%)	0	42 (59%)	29 (41%)	0
4565		NA		9 (56%)	7 (44%)	0	16 (67%)	8 (33%)	0
4744		NA		18 (72%)	7 (28%)	0	16 (67%)	8 (33%)	0

Table 3

Buccal alveolar bone strain (mean and S.D., $\mu\epsilon$) during mastication (sides combined).

Pig	# of Chews	Extraction Side			# of Chews	Occlusion Side		
		Shear	Max (ϵ_1)	Min (ϵ_2)		Shear	Max (ϵ_1)	Min (ϵ_2)
5398	16	381 \pm 190	260 \pm 143	-121 \pm 55	16	957 \pm 398	427 \pm 135	-529 \pm 267
5414	16	215 \pm 81	146 \pm 96	-66 \pm 47	16	289 \pm 187	180 \pm 71	-109 \pm 58
5536	16	129 \pm 82	81 \pm 52	-48 \pm 34	17	259 \pm 102	130 \pm 63	-128 \pm 55
5545		No data			16	457 \pm 213	165 \pm 59	-293 \pm 193
4744	24	224 \pm 108	190 \pm 129	-35 \pm 35	41	355 \pm 79	264 \pm 46	-89 \pm 51
4565	27	454 \pm 94	286 \pm 90	-168 \pm 25	27	511 \pm 154	190 \pm 52	-321 \pm 109
Mean \pm S.D.		281 \pm 133	193 \pm 83	-88 \pm 56		471 \pm 257	226 \pm 108	-245 \pm 171
P values*		0.04	.4	.06				
Extraction vs. Occluding								

Max = tension; Min = compression; Shear = Max + Min (absolute value).

* Wilcoxon signed rank test

Table 4

M₁ specimen stiffness, mean ± standard deviation.

Tissue origin	Low Load Stiffness (Mpa)	High Load Stiffness (Mpa)
Extraction side M ₁	344 ± 101	935 ± 294
Occluding side M ₁	668 ± 183	1117 ± 443
<i>p</i> -value, extraction vs. occluding n=6	p=0.04	p=0.50

Table 5

Alveolar bone microstrain in $\mu\epsilon$ at buccal, lingual and crypt gages at 440 and 890N.

	Buccal Gage			Lingual Gage			Crypt Gage		
	Shear	Max (ϵ_1)	Min (ϵ_2)	Shear	Max (ϵ_1)	Min (ϵ_2)	Shear	Max (ϵ_1)	Min (ϵ_2)
Extraction side									
440N									
Mean	297	17	-281	796	213	-583	614	330	-284
S.D.	150	55	131	763	125	668	454	186	275
890N									
Mean	569	27	-542	1370	337	-1034	1031	560	-471
S.D.	266	100	248	1379	216	1195	724	272	460
Occluding side									
440N									
Mean	293	42	-251	479	130	-349	575	212	-364
S.D.	210	70	177	324	161	191	303	204	138
890N									
Mean	507	73	-435	830	217	-613	1028	389	-639
S.D.	405	133	324	567	284	320	569	364	247
P values*									
Extraction vs. Occluding									
440N	0.9	0.08	0.3	0.9	0.7	0.9	1.0	0.5	0.5
890N	0.7	0.04	0.1	0.9	0.9	0.9	0.7	0.5	0.5

Max = tension; Min = compression; Shear = $\epsilon_1 - \epsilon_2$.

* Wilcoxon signed rank test

Table 6

Mineralization apposition rates ($\mu\text{m}/\text{day}$) for extraction and occluding side alveolar bone.

	Prefunctional MAR (Between 1st and 2nd markers)			Functional MAR (Between 3rd and 4th markers)			Full Occlusion MAR (Between 4th marker and osteoid)		
	Mesial	Inter-radicular	Distal	Mesial	Inter-radicular	Distal	Mesial	Inter-radicular	Distal
Extraction side	71 \pm 14	103 \pm 33	78 \pm 32	278 \pm 82	204 \pm 65	71 \pm 16	225 \pm 60	256 \pm 98	113 \pm 37
Occluding side	86 \pm 63	129 \pm 20	56 \pm 18	115 \pm 38	156 \pm 30	61 \pm 7	149 \pm 51	161 \pm 64	105 \pm 18
P values* n=4	0.6	0.4	0.4	0.06	0.2	0.3	0.2	0.07	0.8

* paired t-test